

A Rigid Molecular Scaffold Affixing a (Polypyridine)ruthenium(II)- and a Nickel(II)-Containing Complex: Spectroscopic Evidence for a Weakly Coupled Bichromophoric System

Yann Pellegrin,^[a] Katja E. Berg,^[a] Geneviève Blondin,^[a] Elodie Anxolabéhère-Mallart,^[a] Winfried Leibl,^[b] and Ally Aukauloo*^[a]

Keywords: Ruthenium / Nickel / Polynuclear complexes / Rigid heteroditopic ligands / Redox chemistry / Photophysical studies

The synthesis of DppztBuSalH₂ (**7**), a rigid conjugated ditopic ligand containing a Dppz (dipyrido[3,2-*a*:2',3'-*c*]phenazine) skeleton and a salophen-type chelate, is reported. The complexes DppztBuSalNi (**10**), [Ru(bpy)₂(DppztBuSalH₂)]²⁺ (**11**), and [Ru(bpy)₂(DppztBuSalNi)]²⁺ (**12**) have been prepared and characterised using common spectroscopic methods. Electrochemical, UV/Vis spectroelectrochemical and EPR studies were conducted on compounds **7**, **10**, **11**, and **12**. The singly reduced radical forms of **7** and **10** can be generated electrochemically, with the lone electron located on the low-lying phenazine π^* -molecular orbital. Complexes **11** and **12** show several reduction waves and electronic and EPR data obtained for the electrogenerated singly reduced species show them to be closely related to the radical species **7**⁻ and

10⁻, respectively. The presence of nickel(II) in compound **12** renders the addition of the second electron on the phenazine group reversible. Both **11** and **12** show common features on the cathodic side of their cyclic voltammograms, with reversible one-electron ruthenium-centred oxidation. An additional low-potential reversible-oxidation wave is observed for **12**, and this is ascribed to oxidation of the nickel(II) ion. The combined spectroscopic data best describe the ruthenium-containing complexes as weakly coupled bichromophoric systems. Photophysical studies attest to the formation of a charge-separated state for **11**, whereas a strong quenching is detected for **12**.

(© Wiley-VCH Verlag GmbH & Co. KGaA, 69451 Weinheim, Germany, 2003)

Introduction

Ruthenium complexes such as [Ru(bpy)₃²⁺], which contain α,α' -diimine ligands, have repeatedly intrigued chemists due to their unique photophysical properties.^[1] These lumophores have been widely used in studies of photochemically or electrochemically induced multielectron or energy transfers.^[2] More recently, a wide variety of complexes bearing the Ru(bpy)₃²⁺ unit have been designed with the aim of devising a new class of anion and cation sensors.^[3] In such “molecular reconnaissance machines” the response is triggered by a modification of the luminescence and/or electrochemical properties of the photoactive core in the presence of the substrate. Molecular switches using this lumophore take advantage of this fundamental characteristic of the [Ru(bpy)₃²⁺] core.^[4] In general, the recent extensive developments in the area of inorganic photochemistry can be credited to the well-known metal-to-ligand charge transfer

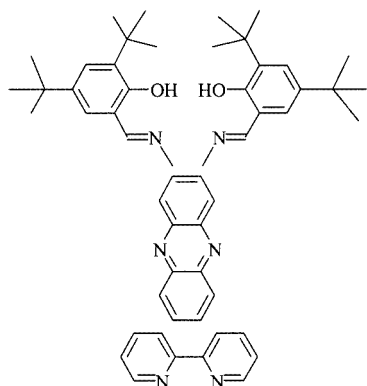
(MLCT) bands of [Ru(bpy)₃²⁺]; excitation of this complex at wavelengths corresponding to these bands leads to the formation of the lowest-energy excited state corresponding to [Ru^{III}(bpy)⁻(bpy)₂]²⁺.^[5] This energetic excited state has been exploited to serve both as an electron-transfer reductant and an oxidant.^[6] In this respect, research on mixed-metal dimetallic systems containing both ruthenium and a first-row transition metal ion was triggered due to their potential in the study of electron transfer^[7] and in the development of novel photocatalysts.^[8] At the forefront of this research is the design of suitable ligands capable of coordinating the ruthenium centre and the transition metal ion. A great number of homoditopic ligands and complexes thereof have been synthesised, and electron and energy transfers have been studied in relation to the chemical nature of the complexes and the intermetallic separation provided by the spacer.^[9] The 2,2'-bipyridine ligand has been extensively used as the starting point in the synthesis of a considerable number of functionalised heterotopic ligands.^[10] In most cases however, bipyridine is covalently linked to an ancillary ligand by a flexible arm. In such systems, the distance between, and the orientation of, the electron donor and acceptor, parameters which are essential in electron transfer studies, are not known precisely.^[11] In addition, it has been shown that photophysical properties are a function of the

^[a] Laboratoire de Chimie Inorganique, UMR 8613, Université de Paris-Sud, 91405 Orsay, France
E-mail: aukauloo@icmo.u-psud.fr

^[b] Service de Bioénergétique, CEA Saclay, Bât. 532, 91191 Gif-sur-Yvette CEDEX, France

Supporting information for this article is available on the WWW under <http://www.eurjic.org> or from the author.

position of the pendant ligand on the bipyridine moiety.^[12] With these considerations in mind, we have devoted our attention to the synthesis of rigid conjugated hybrid ligands capable of holding the two protagonist metal ions with known intermetallic distances.^[13] We report here the synthesis of the novel heteroditopic ligand DppztBuSalH₂ (**7**) based on the Dppz^[14] (dipyrido[3,2-*a*:2',3'-*c*]phenazine) skeleton which contains a salophen-type cavity. This ligand can be viewed as a fused ring system of bipyridine, phenazine and salophen.

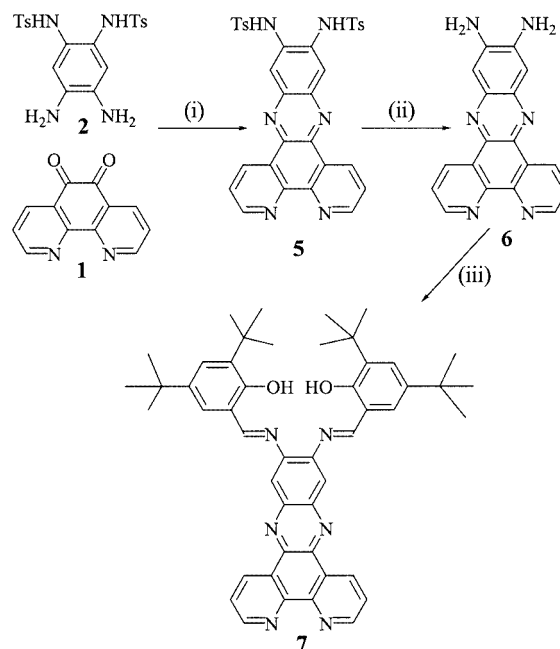


The coordinating ability of **7** is demonstrated by the stepwise metallation of both anchoring sites leading to a new ruthenium/nickel complex. Electrochemical studies coupled with UV/Vis/NIR and EPR techniques have been used to elucidate the redox behaviour and nature of the electro-generated species derived from the complexes [Ru(bpy)₂(DppztBuSalH₂)]²⁺ (**11**) and [Ru(bpy)₂(DppztBuSalNi)]²⁺ (**12**). These results have been corroborated by comparative studies carried out on the unmetallated ligand **7** and the mononuclear nickel(II) complex [DppztBuSalNi] (**10**), in which the phenanthroline end of the ligand is metal-free. The synthesis of this latter complex and the study of its electronic properties were necessary in order to shed light on the actual contribution of each chromophore in the dinuclear ruthenium/nickel complex. The results of these studies suggest a weakly coupled bichromophoric complex, and that the ligand participates actively in the electrochemical processes of the mono- and dinuclear compounds. Finally, results from preliminary photophysical studies are given.

Results and Discussion

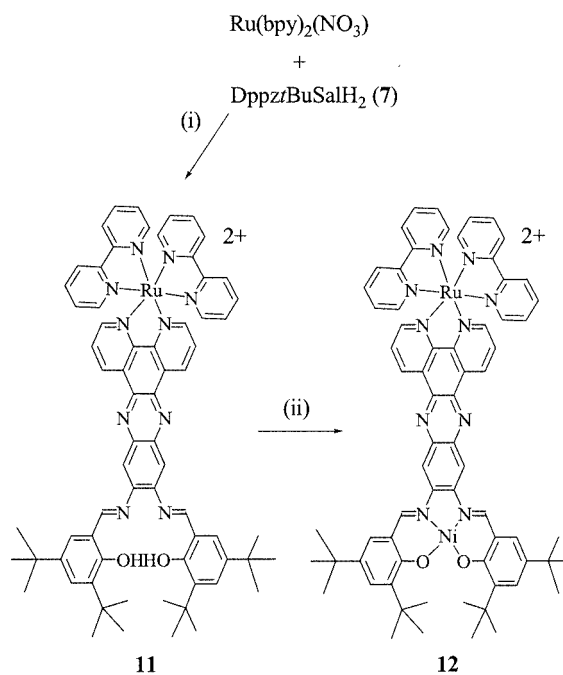
Synthesis

The synthetic pathway for **7** is shown in Scheme 1. Condensation of phendione **1** with 1,2-diamino-4,5-bis(*p*-tosylamino)benzene (**2**) in refluxing methanol gave **5** in quantitative yield. Deprotection of the tosyl groups was carried out in concentrated sulfuric acid to give **6** in near quantitative yield. Our synthetic approach leading to **6** differs from the one described by Lehn et al^[20] in that no further purifi-



Scheme 1. Synthetic route for the preparation of the ligand DppztBuSalH₂ (**7**); conditions: (i) reflux in MeOH; (ii) concd. H₂SO₄, room temp., Na₂CO₃; (iii) reflux in EtOH/HC(OEt)₃

cation was necessary prior to use. Bearing in mind the solubility problems encountered with rigid conjugated systems, we intentionally synthesised the corresponding Schiff base by condensation of 2 equiv. of 3,5-di-*tert*-butylsalicylaldehyde in the presence of triethyl orthoformate in boiling ethanol. Selective metallation (Scheme 2) of the different coordinating sites of **7** was achieved by initially coordi-



Scheme 2. Selective metallation of DppztBuSalH₂; (i) reflux in MeOH, NH₄PF₆ (aq); (ii) Ni(acetate)₂·4H₂O reflux in MeOH, NH₄PF₆ (aq)

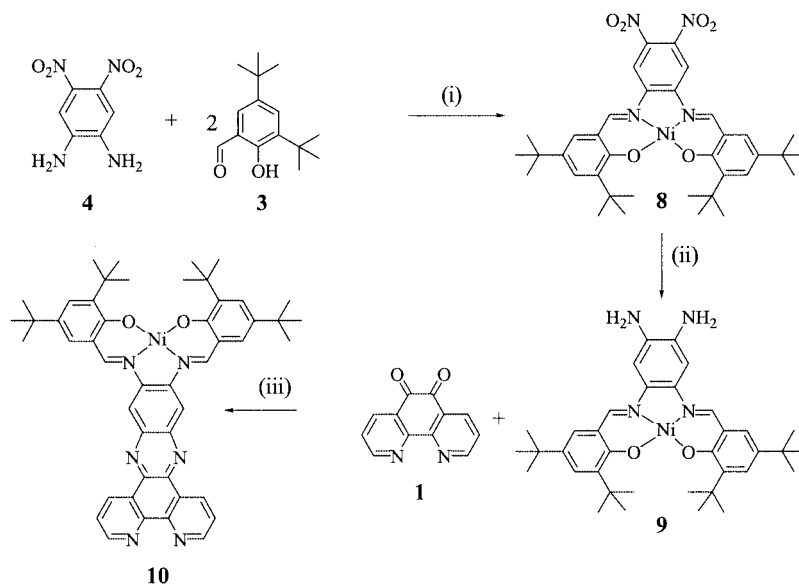
nating the phenanthroline end to $[\text{Ru}(\text{bpy})_2]^{2+}$. The salophen cavity of the resulting complex $[\text{Ru}(\text{bpy})_2(\text{DppztBuSalH}_2)^{2+}]$ (**11**) was easily metallated using nickel(II) acetate according to usual procedures.^[36] Compounds **11** and **12** were purified for photophysical measurements, by chromatography on a neutral alumina column using dichloromethane/methanol (95:5 and 90:10, respectively) as eluents, and the desired compounds were collected as the first major fraction in both cases.

The synthetic pathway for **7** is shown in Scheme 1.

A different synthetic strategy was required to prepare $[\text{DppztBuSalNi}]$ (**10**), the complex containing Ni^{II} in the salophenic cavity (see Scheme 3). Direct complexation of the salophenic cavity was discarded as it results in the formation of polynuclear Ni^{II} complexes and purification of the mixture was arduous and gave only low yields. As an alternative we used the well-known template synthesis to prepare the Ni^{II} complex **8** in almost quantitative yield.^[21] Reduction of the nitro groups was carried out under hydrogen in the presence of Pd/C as catalyst. Complex **10** was synthesised in good yield following the condensation of the diamino derivative **9** with phendione **1** in refluxing methanol.

^1H NMR Spectra

^1H NMR spectroscopy was used to monitor the stepwise metallation of **7**. Attachment of the N–N chelating site of the phenanthroline end to the diamagnetic Ru^{II} showed, as expected, a downfield shift of the phenanthroline protons and certain bipyridine protons.^[22–23] This phenomenon was even more pronounced when the Ni^{II} ion was bound in the tetracoordinating salophen cavity, with a downfield shift of as much as $\delta = 0.95$ ppm for the signal of the imine hydrogen atoms. Evidence for the coordination of nickel(II) to the salophen cavity was also obtained from ^1H NMR spectroscopy, with loss of the signal from the phenol protons.



Scheme 3. Synthetic steps for DppztBuSalNi (**10**); (i) $\text{NiCl}_2 \cdot 6\text{H}_2\text{O}$, reflux in dry ethanol/ $\text{HC}(\text{OEt})_3$; (ii) H_2 40 atm, Pd/C in MeOH; (iii) reflux in MeOH

Infrared Spectra

The sequential binding of the different metal ions was also monitored by infrared spectroscopy. Coordination of ruthenium was characterised by aliphatic C–H vibrations of the *tert*-butyl groups in the region of 2950 cm^{-1} , together with intense absorption bands at about $1585\text{--}1610\text{ cm}^{-1}$ corresponding to the imino C=N stretch. Nickel(II) insertion to yield **12** was indicated by a red shift of about 30 cm^{-1} for the band of the imino groups.^[24]

Mass Spectrometry

Mass spectra of the ruthenium complexes **11** and **12** were obtained by Electrospray Ionisation Mass Spectrometry. Parent ion peaks minus one or two accompanying anions were detected. In both cases, the doubly charged species appeared as the major peak. The experimental and the simulated spectra for the doubly charged complex $[\text{12} - 2\text{PF}_6]^{2+}$ are given in Figure 1.

UV/Vis Spectroscopy

The absorption spectra of **7**, **10**, **11** and **12** in CH_2Cl_2 are shown in Figure 2, and the absorption maxima together with their extinction coefficients given in Table 1. Figure 2 (a) shows the electronic perturbation that occurs upon metallation of the salophenic N_2O_2 cavity of **7** with Ni^{II} . Strong $\pi\text{-}\pi^*$ transitions at 310 and 430 nm characterise the extended delocalised π -system of the DppztBuSalH_2 skeleton. Spectral modifications for the mononuclear Ni^{II} complex are noticed in both the high- and low-energy regions compared to the free ligand. The prominent feature is the MLCT band at 500 nm typical of Ni–salophen complexes. The dissymmetric nature of this band may suggest the presence of $\pi\text{-}\pi^*$ intra-ligand transitions which undergo a bathochromic shift relative to that of the free ligand. This shift

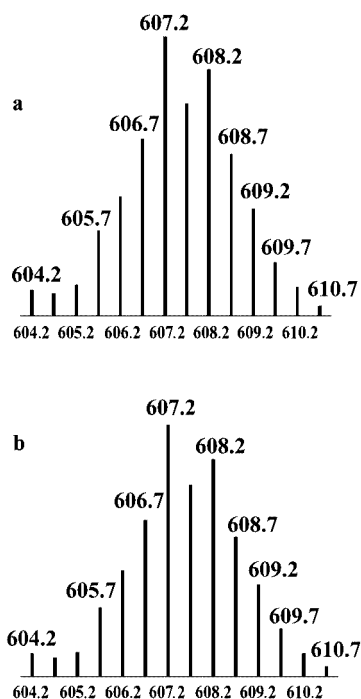


Figure 1. ESI-MS of $[\text{Ru}(\text{bpy})_2\text{DppztBuSalNi}]^{2+}$ (**12**): (a) experimental and (b) simulated spectrum

can be attributed to a diminution of the HOMO–LUMO gap upon metallation. The weak absorption band observed at the base of the MLCT transition at 620 nm corresponds to a d-d transition for Ni^{II} sitting in a square-planar coordination site.^[25]

UV/Vis spectra of **11** and **12** are depicted in Figure 2 (b). The electronic absorption spectrum of **11** contains spectral features due to both $[\text{Ru}(\text{bpy})_3]^{2+}$ and DppztBuSalH_2 . Two intense bands are observed at higher energy, one for the usual intense spin-allowed ligand-centred transitions of the bpy ligands at 290 nm characteristic of (polypyridine)-ruthenium complexes^[1,5] and a band at 325 nm attributed to intra-ligand transitions of **7**. A broad, asymmetric absorption band extending from 390 to 550 nm is accounted for by the superposition of low-energy π - π^* intra- DppztBuSalH_2 -ligand transitions and an admixture of $d\pi(\text{Ru})-\pi^*(\text{bpy})$ together with $d\pi(\text{Ru})-\pi^*(\text{bpy}')$ (where bpy' denotes the bipyridine moiety of the ligand **7**) MLCT transitions. This agrees with previous findings for (polypyridine)ruthenium(II) complexes containing extended delocalised π -systems, where it has been shown that the low-lying orbitals confined on the central part of the rigid aromatic ligand are decou-

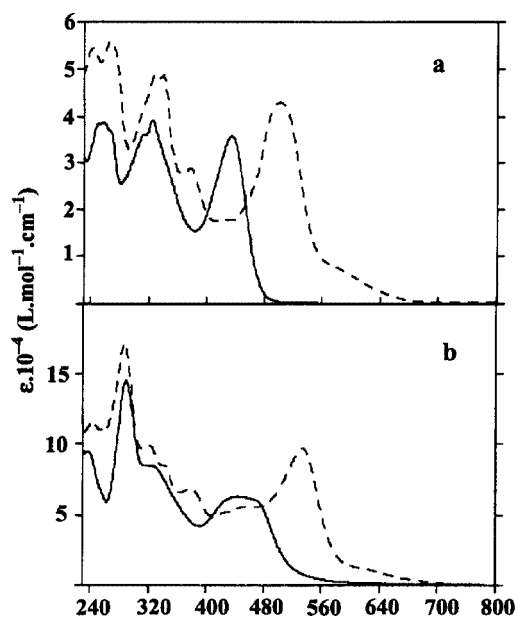


Figure 2. Absorption spectra in CH_2Cl_2 ; a) DppztBuSalH_2 (**7**) (solid line) and DppztBuSalNi (**10**) (dotted line); b) spectra of $[\text{Ru}(\text{bpy})_2\text{DppztBuSalH}_2]^{2+}$ (**11**) (solid line) and $[\text{Ru}(\text{bpy})_2\text{DppztBuSalNi}]^{2+}$ (**12**) (dotted line)

pled from the metal t_{2g} -type orbitals^[26] due to the nearly non-existent orbital contribution from the nitrogen atoms of the coordinating imino groups. Hence, the optical properties of **11** suggest a bichromophoric character for the complex. Metallation of the salophen cavity with Ni^{II} induces a significant change in the appearance of the electronic absorption spectrum as shown in Figure 2 (b). The position and intensity of the π - π^* transitions due to the bpy moieties are almost unaffected. A series of three bands between 320 and 380 nm, probably originating from intra-ligand π - π^* transitions together with charge transfer transitions from Ni^{II} to the ligand, is observed. This explanation is supported by the observation of these bands in the spectrum of complex **10**. Ruthenium charge transfer transitions towards π^* -orbitals of the ligands are detected as a shoulder at 460 nm on a more intense MLCT band from the salophen–Ni part of the dinuclear Ru/Ni complex **12**. The observation of a weak band at ca. 620 nm, characteristic of a d-d transition for a d^8 square-planar Ni^{II} complex, provides further evidence for metallation of the salophen cavity.

Spectroelectrochemical Properties and EPR Spectroscopy

Electrochemical studies on $[\text{Ru}(\text{diimine})_3]^{2+}$ complexes are widely used to characterise the π^* -orbital energies of

Table 1. UV/Vis/NIR data for DppztBuSalH_2 (**7**), DppztBuSalNi (**10**), $[\text{Ru}(\text{bpy})_2\text{DppztBuSalH}_2]^{2+}$ (**11**) and $[\text{Ru}(\text{bpy})_2\text{DppztBuSalNi}]^{2+}$ (**12**)

	λ [nm] (ϵ [10^{-3} $\text{L}\cdot\text{mol}^{-1}\cdot\text{cm}^{-1}$])							
DppztBuSalH_2 (7)	250 (38.4)	260 (38.7)	265 sh	310 (36.3)	325 (39.1)	345 sh	430 (35.8)	
DppztBuSalNi (10)	245 (54.6)	265 (55.7)	330 (49)	340 (48.8)	375 (28.6)	430 sh	500 (42.8)	
$[\text{Ru}(\text{bpy})_2(\text{DppztBuSalH}_2)]^{2+}$ (11)	240 (94.4)	290 (145)	325 sh	445 (63.1)	465 sh			
$[\text{Ru}(\text{bpy})_2(\text{DppztBuSalNi})]^{2+}$ (12)	245 (116)	290 (172)	320 (99.1)	340 (85.1)	380 (68.6)	455 sh	535 (97.3)	620 sh

Table 2. Half-wave potentials E for the oxidation ($^{\text{ox}}E$) and the reduction ($^{\text{red}}E$) of DppztBuSalH₂ (**7**), [DppztBuSalNi] (**10**), [Ru(bpy)₂DppztBuSalH₂]²⁺ (**11**) and [Ru(bpy)₂DppztBuSalNi]²⁺ (**12**) (from cyclic voltammetry at 100 mV/s; $E = 1/2(E_{\text{pa}} + E_{\text{pc}})$ in V vs. SCE in the presence of TBAClO₄)

	$^{\text{v}}E$	$^{\text{IV}}E$	$^{\text{III}}E$	$^{\text{II}}E$	$^{\text{I}}E$	$^{\text{i}}E$	$^{\text{ii}}E$	$^{\text{iii}}E$
DppztBuSalH ₂ (7) ^[a]				-1.40 ^[b]	-1.11	+1.18	+1.29 ^[c]	+1.58 ^[c]
[DppztBuSalNi] (10) ^[a]				-1.43 ^[b]	-0.99	+1.13		
[Ru(bpy) ₂ DppztBuSalH ₂] ²⁺ (11) ^[d]		-2.0 ^[b]	-1.63	-1.45	-0.88	+1.26 ^[c]	+1.43 ^[c]	
[Ru(bpy) ₂ DppztBuSalNi] ²⁺ (12) ^[d]	-1.88 ^[b]	-1.64	-1.44	-1.27	-0.81	+1.07	+1.29 ^[c]	+1.42 ^[c]

^[a] Measured in dichloromethane. ^[b] Measured in acetonitrile. ^[c] Partly irreversible step, cathodic peak given. ^[d] Irreversible step, anodic peak given. ^[e] Adsorption and desorption phenomena observed under our experimental conditions, anodic peak given.

Table 3. UV/Vis/NIR data for the electrogenerated species (from spectroelectrochemistry)

	λ [nm] (ϵ [10^{-3} L·mol ⁻¹ ·m ⁻¹])									
DppztBuSalH ₂ ⁻ (7 ⁻)	300 (32.5)	381 (32.4)	455 (18.1)	545 sh	750 sh	840 (10)				
[DppztBuSalNi] ⁻ (10 ⁻)	308 (36.3)	326 (35.8)	372 (42.4)	390 sh	490 sh	517 (38.1)	613 (10.5)	820 sh	917 (17.1)	
[Ru(bpy) ₂ DppztBuSalH ₂] ⁺ (11 ⁺)	245 (95.4)	291 (145)	382 (73.8)	470 (56.2)	550 sh	750 (14.7)	880 sh			
[Ru(bpy) ₂ DppztBuSalNi] ⁺ (12 ⁺)	244 (135)	289 (169)	353 (79)	388 (82.3)	475 sh	515 (80)	622 sh	800 sh	865 (23.4)	

the ligands linked to Ru^{II}. In addition, the redox potential of the Ru^{III/II} metal centre gives, in general, a clear indication of the nature of the interaction with the coordinated ligands. Furthermore, electrochemical data coupled with other spectroscopic information are currently used to rationalise the modifications in the absorption and emission spectra of [Ru(diimine)₃²⁺] derivatives.^[1b,14c,27] The electrochemical properties of **7**, **10**, **11** and **12** were investigated by

cyclic voltammetry (CV) and these data are summarised in Table 2. Electronic data for the electrochemically generated species are given in Table 3. In what follows, we analyse the electrochemical behaviour of **7** and **10** and discuss the spectroscopic characterisation of the electrogenerated species. These results are then correlated to the Ru^{II}-containing complexes.

Ligand DppztBuSalH₂ (**7**) and Complex [DppztBuSalNi] (**10**)

The cyclic voltammograms of the free ligand **7** and its Ni^{II} complex **10** are shown in Figure 3 (a). Owing to the poor solubility of these species in acetonitrile, cyclic voltammograms of **7** and **10** were run in dry dichloromethane. Two waves are observed upon reduction of **7**, one reversible and a second quasi-irreversible at -1.1 and -1.39 V vs. SCE, respectively. The reversible one-electron reduction wave at -1.1 V falls in the range of potentials typical for phenazine-containing moieties.^[27] No reversible waves are observed upon oxidation, even when scanning up to +1.7 V. However, two consecutive poorly resolved waves at +1.18 and +1.29 V vs. SCE are attributed to oxidation of the phenol groups. Compared to the first reduction of Dppz, an anodic shift of about 100 mV indicates the uptake of the first electron by the “modified” phenazine framework which contains imino π -accepting groups. The second electron addition occurs at a more positive potential than that of Dppz [-1.4 vs. -2.0 V (SCE), respectively]. The fact that salophen lacks a reduction wave within this potential range clearly implies that this electron-transfer process involves the phenazine part of the ligand. As reported earlier, the doubly reduced form of the Dppz ligand leads to a considerable increase in charge at the nitrogen atoms, thus enhancing its protonation aptitude. In the case of **7**, the same phenomenon will be occurring and this explains the flat-

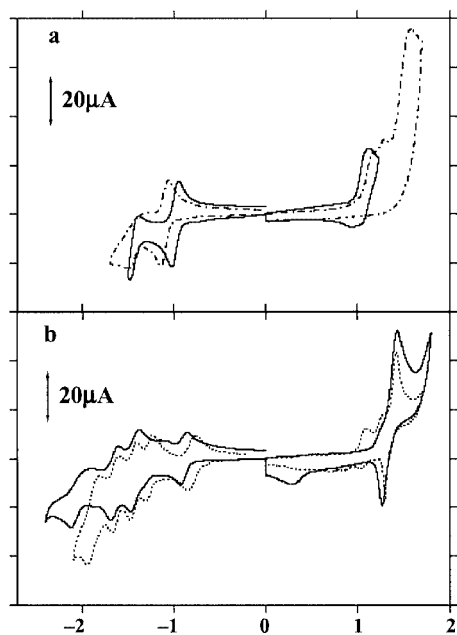


Figure 3. Cyclic voltammograms in CH₂Cl₂ (10⁻³ M solutions, room temperature, sweep rate 100 mV·s⁻¹, Ag/AgClO₄ electrode as reference, 0.1 M TBAClO₄ as supporting electrolyte); a) DppztBuSalH₂ (**7**) (dotted line) and DppztBuSalNi (**10**) (solid line); b) [Ru(bpy)₂DppztBuSalH₂]²⁺ (**11**) (solid line) and [Ru(bpy)₂DppztBuSalNi]²⁺ (**12**) (dotted line)

tened nature of the corresponding anodic peak.^[28] Redox properties of **10** are illustrated in Figure 3 (a, solid line); in comparison to **7** only minor changes are observed upon reduction. A shift of about 120 mV towards less negative potential is noticed for the first reversible reduction wave. The increased ease of reduction of the nickel(II) complex confirms the lowering in energy of the ligand LUMO upon metallation. In contrast to the ligand, a reversible oxidation wave is observed at +1.13 V vs. SCE, which is attributed to the formation of a nickel(III) complex. Such a potential is consistent with the Ni^{III/II} redox couple of Ni–salophen.^[29]

Spectroelectrochemical studies were carried out to investigate the stability and the spectroscopic signatures of electroreduced **7** and **10** after the first reduction wave. UV/Vis/NIR spectral changes of **7** and **10** were monitored at room temperature by using a thin-layer cell in dry dichloromethane in the presence of 0.1 M TBAPF₆ at –1.2 and –1.0 V, respectively. The electronic response of **7** is strongly modified upon addition of the first electron, as shown in Figure 4 (a). New high-intensity broad bands spanning the range 600–950 nm and another broad band at 380 nm are observed. These new spectral features are also found for singly reduced phenazine-containing compounds.^[27] The double-hump band observed for Dppz[–] (547 and 570 nm) is shifted to lower energy for **7**[–] with the maxima at 765 and 840 nm, indicating that the unpaired electron is localised on a more extended π -system.

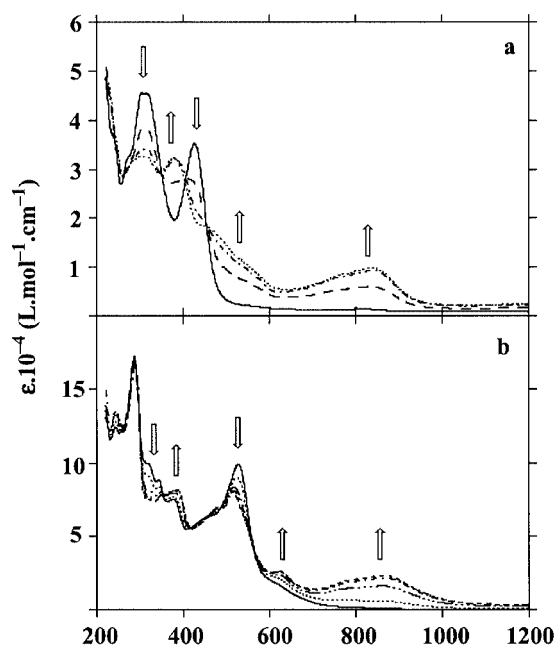


Figure 4. Electronic absorption spectra upon electrolysis at controlled potential in CH₂Cl₂ (10^{–3} M solutions, room temperature, SCE as reference, 0.1 M TBAClO₄ as supporting electrolyte); a) DppztBuSalH₂ (**7**) upon reduction at –1.3 V/SCE; b) [Ru(bpy)₂DppztBuSalNi]²⁺ (**12**) upon reduction at –0.96 V/SCE

The complete recovery of the initial spectrum upon reoxidation, together with the observation of several isosbestic points (265, 350, 405 and 450 nm), confirmed the presence of only two species in equilibrium at all times during the

electrochemical study, showing the reversible nature of this electron-transfer process under our experimental conditions. The singly reduced species was also generated by a controlled potential bulk electrolysis at –30 °C. The EPR spectrum of the electrolysed solution showed an isotropic signal at $g = 2.007$, indicating the presence of an organic radical species with a peak to trough line width of 0.75 mT. In contrast to the paramagnetic singly reduced Dppz species, where well-resolved EPR signals have been observed,^[27] the smooth EPR signal registered for **7**[–] confirms the delocalisation of the electron on a more delocalised π -system, hence resulting in the interaction of the single electron with a larger number of nuclear spins.

The spectroelectrochemical behaviour of **10** was monitored using identical techniques as for **7**. The changes in the electronic spectrum of **10** upon the addition of one electron are similar to those of **7**, at least in the low-energy region. However, the maxima of these broad bands are shifted to lower wavenumbers (ca. 1040 cm^{–1}) indicating a smaller energy difference between the HOMO and LUMO when Ni^{II} is inserted into the N₂O₂ coordinating cavity. These absorption bands resemble those observed for the monoanion radical of **7** which favours localisation of the added electron on the phenazine part of the metallo complex. No substantial change in the d-d transition of the Ni^{II} centre at 620 nm is observed, but this band becomes more apparent in the electrolysed species. The one-electron process for this reduction wave was confirmed by bulk electrolysis at a controlled potential, and a reverse cyclic voltammogram on the electrolysed solution indicates the presence of only one species at the same potential as the initial complex. The frozen solution EPR spectrum of the electrolysed compound is shown in Figure 5. The signal is slightly anisotropic and is best simulated with values of $g_{\perp} = 2.0055$ and $g_{\parallel} = 2.0012$. This weak anisotropy can be explained by a partial delocalisation of the lone electron in a d _{π} -type orbital of the nickel centre.^[30] The lack of hyperfine coupling is most probably due to extensive overlap of a large number of signals with small EPR coupling constants, resulting from interaction with neighbouring atoms.

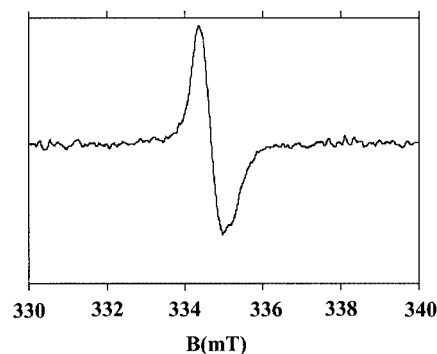


Figure 5. EPR spectra of [DppztBuSalNi][–] (**10**[–]) at 100 K after bulk electrolysis at –1.2 V vs. SCE in dry dichloromethane and TBAClO₄ as supporting electrolyte

[Ru(bpy)₂DppzrBuSalH₂]²⁺ and [Ru(bpy)₂DppzrBuSalNi]²⁺ Complexes

Electrochemical properties of the ruthenium-containing complexes have been studied in both dichloromethane and acetonitrile in the presence of 0.1 M TBAP as supporting electrolyte, and the corresponding data are given in Table 2. Electrochemical studies of [Ru(diimine)₃²⁺] complexes are indeed crucial in evaluating the relative energy of the ligand π*-orbitals, especially for heteroleptic complexes, and also the nature of the interactions of the ligands with the metal centre. The first reductive process for the metal complex is often informative regarding the energy levels of the π*-orbitals of the ligands linked to the ruthenium(II) ion, whereas the first oxidation process is indicative of the metal t_{2g}-orbital energy. However, this is only true if the processes of reduction and oxidation are as in Equations 1 and 2, respectively.^[31]



Cyclic voltammograms of **11** and **12** are given in Figure 3 (b). The electrochemical behaviours of **11** and **12** may be regarded as the superposition of each of **7** and **10** together with the [Ru(bpy)₃²⁺] chromophore, respectively. On the cathodic side of the CV of **11**, both reduction waves for the ligands are observed at -0.89 and -1.3 V vs. SCE, followed by the sequential addition of one electron to the bipyridine co-ligands. The oxidation wave for the Ru^{III/II} couple is observed at +1.4 V vs. SCE and is probably masking the oxidation wave for the phenol groups. The fact that the oxidation potential for the Ru^{II} ion remains unchanged when compared to [Ru(bpy)₃²⁺] supports the idea that the phenazine moiety together with the bis(salicylidene)diimine groups have very little electronic influence on the metal centre. One can thus envision [Ru(bpy)₂DppzrBuSalH₂]²⁺ as consisting of two chromophores with little electronic communication between them. Complex **12** displays similar electrochemical behaviour; an almost identical pattern is observed on the cathodic part of the CV while on oxidation, a reversible wave is observed at +1.07 V vs. SCE followed by another wave at 1.42 V vs. SCE corresponding to oxidation of the phenol group, which is detected as a shoulder on the oxidation wave for the Ru^{III/II} couple. It should be noted that, when scanning up to 1.8 and 1.7 V for **11** and **12**, respectively, we observed irreversible cathodic waves at 0.28 V for **11** and 0.37, 0.70 and 0.86 V for compound **12**. These waves probably originate from chemically altered species as no such waves are present when scanning to a potential just beyond the Ru^{III/II} couple. The intensities of the corresponding waves for the Ru^{III/II} couple suggest that adsorption and desorption phenomena are taking place at the surface of the vitreous carbon electrodes.

Singly Reduced Forms of [Ru(bpy)₂DppzrBuSalH₂]²⁺ (11**) and [Ru(bpy)₂DppzrBuSalNi]²⁺ (**12**)**

The first reduction potential for **11** occurs at -0.99 V which is very close to that of the free ligand under the same conditions (-1.11 V) [¹E(complex) - ¹E(ligand) = 0.12 V].^[26,27] This implies that the coordination of ligand **7** to the Ru^{II} ion has little influence on the uptake of the first electron. Another way to describe this result is to consider that the singly occupied molecular orbital (SOMO) is developed mainly on the phenazine together with the bis(salicylidene)diimine framework. Moreover, the displacement of this wave to a more positive potential can be related to the dipositive charge of the complex of ligand **7**. Spectroelectrochemically, the uptake of the first electron is characterised by the growth of intense bands in the region of 600 to 950 nm and at 380 nm, attributable to the coordinated DppzrBuSalH₂. Similarly to **7**, a fall in intensity of the π-π* intra-ligand charge-transfer transitions at 325 and 440 nm for **11** also underpins the proposed site of reduction. In addition, no alteration in either the Ru^{II} to bpy MLCT transitions at about 460 nm or the internal transition of the bound bpy ligands in their neutral form at 290 nm is observed, thus providing further evidence for the reduction site.^[32]

EPR of a frozen solution of the singly reduced complex **11**^{•+} generated electrochemically showed an isotropic signal with a *g* factor of 2.007. The negligible change in the observed *g* values for the free ligand **7**⁻ and the ruthenium complex **11**^{•+} reflects the feeble interaction of the unpaired electron with the metal ion. It should be noted that the observed *g* values for other [Ru(bpy)₂(L⁻)²⁺] species, where L is a diimine-type ligand, deviate markedly from the *g* value of the metal-free ligand anion radical; this is mainly due to a strong interaction of the unpaired electron with the Ru^{II} ion.^[33] Thus, the EPR spectrum of **11**^{•+} is consistent with the single electron being confined to a molecular orbital located predominantly on part of the ligand skeleton, with a weak contribution from the Ru^{II} centre and the ligating diimine part of the corresponding ligand. As observed in the case of the radical species of the free ligand, no hyperfine structure is observed for **11**^{•+}, probably for the same reason as mentioned above.

The electrochemical response of **12** in acetonitrile is given in Figure 3 (b). Five reversible one-electron reduction waves at room temperature are observed in the potential range scanned. Of particular interest is the approximately 200 mV shift of the first reduction wave to more positive potential relative to **11** and **10**. Such a shift of the redox potential clearly denotes the stabilisation of the LUMO predominantly localised on the phenazine skeleton of the spacer ligand **7**.^[34] The change in the electronic spectrum of **12** upon addition of one electron is shown in Figure 4 (b). The singly reduced species is characterised by the same bands in the low-energy region as those already observed for compounds **7**, **10** and **11** for the same electron transfer process. The spectral modification of **12** is closely related to that of **10**, again confirming the same position for the unpaired elec-

tron of the heterodimetallic complex. No appreciable alteration of the $\pi\text{-}\pi^*$ transition of the chelated bipyridine moieties at 290 nm is observed, and the Ru^{II} -to-ligand charge-transfer transitions at 460 nm are present as shoulders on the pronounced MLCT transitions of the Ni–salophen chromophore. Decisive spectroscopic characterisation of the first reduction process comes from the EPR spectrum of an electrolysed solution of **12**. An isotropic signal with a g factor of 2.013 and a line-to-line width of 0.75 mT typical of a radical species was detected. Here too, no hyperfine coupling is apparent. An interesting feature in the CV of **12** is the presence of a second reversible wave at -1.27 V (in acetonitrile vs. SCE). While no apparent shift has been detected for the second wave of **7** upon metallation of only one end of the heterotopic ligand (i.e. for compounds **10** and **11**), a marked displacement of about 260 mV to more anodic potential is observed in the case of the dimetallic complex. The more reversible nature of the uptake of the second electron on the bridging ligand reflects the gain in stability of the doubly reduced species in the case where both ends of the ligand contain a divalent ion.

Singly Oxidised Form of **12**

The $\text{Ru}^{\text{II}}/\text{Ni}^{\text{II}}$ complex exhibits three oxidation waves in the positive potential region at +1.07, +1.29 and +1.42 V vs. SCE, respectively. When compared to the first oxidation process of **10**, where only the salophen cavity is occupied by Ni^{II} , a small cathodic shift of ca. 60 mV is noted. The observed potential falls within the range expected for the $\text{Ni}^{\text{III/II}}$ couple of a salophen-type complex. Even the small shift observed for **12** is surprising, as a more positive potential for the oxidation of the Ni^{II} centre would be expected for this dicationic complex.^[29] We tentatively rationalise this observation by noting the more π -accepting character of the bridging ligand when both extremities of the latter are metallated. Hence, a stronger ligand field is exerted on the Ni^{II} centre, thereby enhancing its propensity to oxidise. Few changes were observed spectroelectrochemically upon the removal of the first electron. The frozen-solution X-band EPR spectrum of the electrochemically generated $\text{Ru}^{\text{II}}/\text{Ni}^{\text{III}}$ complex at 15 K shows a rhombic symmetry, with a large g tensor anisotropy ($g_x = 2.289$, $g_y = 2.232$, $g_z = 2.022$), which is commonly observed for Ni^{III} complexes in salophen-type environments.^[29] Upon addition of degassed pyridine to the electrolysed solution and subsequent freezing, we obtained the EPR spectrum shown in Figure 6. The new adduct still exhibits a rhombic-type spectrum with superhyperfine couplings in all g regions. The best agreement between the experimental spectrum and the simulated one was obtained using the following parameters: $g_x = 2.1986$, $g_y = 2.1645$, $g_z = 2.0265$; $A_x = 16.34 \times 10^{-4} \text{ cm}^{-1}$, $A_y = 16.10 \times 10^{-4} \text{ cm}^{-1}$, $A_z = 20.43 \times 10^{-4} \text{ cm}^{-1}$. Simulation was realised using a Gaussian profile and line widths of 0.8, 0.7 and 0.6 mT for the x , y and z peaks, respectively. In addition, a signal at $g = 2.0038$ was detected, and attributed to the phenoxyl radical generated during the electrolysis, due to the close proximity of the two oxidation waves ($\text{Ni}^{\text{III}}/\text{Ni}^{\text{II}}$ and PhO^+/PhO). The well-resolved quin-

tuplet at higher magnetic field is the fingerprint of a six-coordinate Ni^{III} species, with two pyridine rings in axial positions and an axial repartition of the spin density on the Ni^{III} centre.

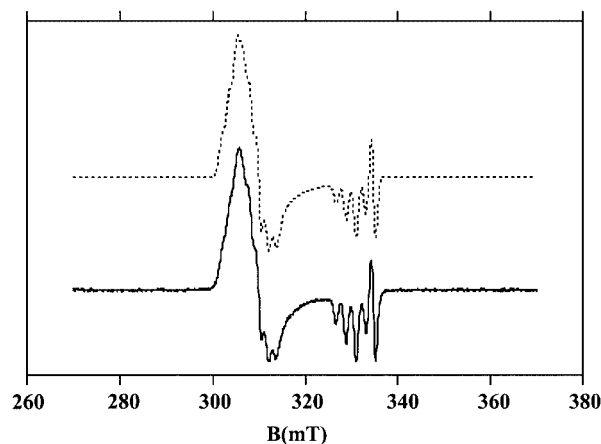


Figure 6. EPR spectrum of $[\text{Ru}(\text{bpy})_2\text{DppztBuSalNi}]^{3+}$ (**12**³⁺) at 15 K, generated by electrolysis at 1.11 V/SCE in dry degassed acetonitrile and 0.1 M TBAClO_4 as supporting salt in the presence of pyridine (solid line); the dotted line shows the simulated spectrum

Preliminary Photophysical Studies

Upon excitation of the mononuclear ruthenium complex **11** at 532 nm (MLCT $\text{Ru}^{\text{II}} \rightarrow$ bipyridine moiety) in degassed ethanol at room temperature, fluorescence emission was observed around 610 nm. The observed fluorescence lifetime (minor of 40 ps is much shorter than that of $[\text{Ru}(\text{bpy})_3]^{2+}$), which indicates rapid quenching of the excited state. Time-resolved absorption spectroscopy revealed that the transient species generated by photoexcitation at 532 nm displays an absorption at around 820 nm, a wavelength similar to that of the electrochemically singly reduced $[\text{Ru}(\text{bpy})_2(\text{DppztBusalH}_2^-)]^{2+}$ species (Figure 4, a). This is a strong indication that the quenching of the excited state is due to internal photoinduced electron transfer, probably forming the charge-separated state $\text{Ru}^{\text{III}}(\text{bpy})_2(\text{DppztBusalH}_2^-)^{2+}$. The lifetime observed for this transient species was about 400 ns. In contrast, the dinuclear complex **12** exhibits a very efficient quenching of the excited state which is not accompanied by absorption changes in the near infrared. The most likely explanation is that fast energy transfer to the Ni^{II} ion occurs in this complex where the excited state is efficiently quenched before internal charge separation can occur. We are currently investigating the photophysical behaviour of **10** and **12** in more detail.

Conclusion

Based on the X-ray structure of **10**^[35] an approximate distance of 12.5 Å between the Ru^{II} and Ni^{II} ions is expected. This separation thus falls within the desired distance for electron or energy transfer studies in these model

complexes. Spectroelectrochemical studies suggest a weak electronic coupling between the different chromophores in our system, a prerequisite in the design of supramolecular systems containing a photoactive site. We believe that our approach to building novel heteroditopic ligands will be a source of inspiration for the synthesis of novel ancillary ligands on anchoring molecules such as phenanthroline.

Experimental Section

General: Electrochemical measurements were performed with an EGG PAR (model 273A) electrochemical workstation. The solvents were distilled under nitrogen in the presence of dry calcium chloride and the solution [$1 \text{ mmol}\cdot\text{L}^{-1}$ for complexes and ligand and $0.1 \text{ mol}\cdot\text{L}^{-1}$ of tetrabutylammonium perchlorate (TBAClO_4)] introduced within an argon-purged heart-shaped cell. Cyclic voltammetry was performed using a glassy carbon electrode (3 mm in diameter) as the working electrode, a platinum grid as the counter electrode and an Ag/AgClO_4 (0.01 M) electrode in acetonitrile as the reference ($E_{\text{ref}} = 0.3 \text{ V}/\text{ECS}$). Electrolyses were carried out at controlled potentials in a three-electrode cell, using a platinum gauze as the working electrode, a platinum grid as the counter electrode and an Ag/AgClO_4 (0.01 M) electrode in acetonitrile as the reference. Low-temperature electrolyses were run using 0.2 M TBA-CIO_4 . UV/Vis/NIR spectra were obtained using 1-cm quartz cells with a Varian Cary 5E spectrophotometer (200–1500 nm). Spectroelectrochemical data were obtained by a combination of a three-electrode thin cell (0.5 mm) mounted in a UV/Vis/NIR spectrophotometer. IR spectra were obtained with a Perkin–Elmer 1000 spectrometer, using KBr matrix pellets. NMR spectra were obtained using Bruker AC 200 (200 MHz) and AC 250 (250 MHz) spectrometers. The solvents used were CDCl_3 or $[\text{D}_6]\text{DMSO}$. EPR spectra were recorded with an X-band Elexsys (Bruker) spectrometer at 15, 77 or 100 K. Elemental analyses were carried out at the Services de Microanalyse, ICSN-CNRS, Gif-sur-Yvette. Mass spectra were recorded with a Finnigan Mat Mat95S in a *BE* configuration at low resolution. Flash-absorption and fluorescence transients were measured with setups of local design. All measurements were taken at 296 K. For absorption transients the measuring light was provided by a 150-W tungsten-halogen lamp, and the wavelength was selected with interference filters placed before and after the $10 \times 1 \text{ mm}$ sealed cuvette containing the sample. The sample was excited at 90° to the measuring beam by a flash from a frequency-doubled Nd:YAG laser (532 nm, duration 5 ns, ca. $2 \text{ mJ}/\text{cm}^2$; Surelight, Continuum). Absorbance changes were detected with a silicon photodiode and signals were amplified by a wideband pre-amplifier (model 5185, EG&G) before they were recorded by a digital oscilloscope (TDS, 744A, Tektronix). For fluorescence transients, excitation was achieved by a flash from a frequency-doubled picosecond Nd:YAG laser (532 nm, duration 25 ps, ca. $300 \mu\text{J}/\text{cm}^2$; Continuum). The detection wavelength was selected by an interference filter centred at 610 nm and signals were detected with a microchannel plate photomultiplier tube (R2566 U, Hamamatsu) and a 7-GHz digitising oscilloscope (IN7000, Intertechnique). Ruthenium trichloride was purchased from the Aldrich Chemical Company. 2,2'-Bipyridine (bpy) and 1,10-phenanthroline (phen) were obtained from the Janssen Chemical Company. 1,10-Phenanthroline-5,6-dione (phendione, **1**),^[15] 1,2-diamino-4,5-bis(*p*-toluenesulfamido)benzene (**2**),^[16] 3,5-di-*tert*-butylsalicylaldehyde (**3**),^[17] 4,5-diamino-1,2-dinitrobenzene (**4**),^[18] and $[\text{Ru}(\text{bpy})_2\text{Cl}_2]$ ^[19] were synthesised as described in the literature.

Synthesis of 11,12-Bis(*p*-tosylamino)dipyrido[3,2-*a*:2',3'-*c*]phenazine (5**):** 1,2-diamino-4,5-bis(*p*-tosylamino)benzene (**2**) (2.23 g, 5 mmol) was added to a suspension of phendione (**1**) (1.55 g, 5 mmol) in methanol (50 mL), and the mixture was refluxed for 1 h. The hot suspension was filtered while hot to give a beige solid which was washed with cold methanol and dried under vacuum. Yield: 2.92 g (94%). IR: $\tilde{\nu} = 3436$ (N–H), 3034, 2820 (C–H), 1619 (C=N), 1580 (C=N) cm^{-1} . ^1H NMR ($[\text{D}_6]\text{DMSO}$): $\delta = 9.48$ (d, 2 H), 9.16 (d, 2 H), 7.93 (dd, 2 H), 7.86 (s, 2 H), 7.78 (d, 2 H), 7.36 (d, 2 H), 2.28 (s, 6 H) ppm. $\text{C}_{32}\text{H}_{24}\text{N}_6\text{O}_4\text{S}_2$ (620.7): calcd. C 61.92, H 3.90, N 13.54; found C 61.88, H 3.82, N 13.42.

Synthesis of 11,12-Diaminodipyrido[3,2-*a*:2',3'-*c*]phenazine (6**):** De-protection of the tosyl group was achieved by treating **5** (1.24 g, 2 mmol) with concentrated sulfuric acid (10 mL) at room temperature for 4 h. The deep violet solution was then added dropwise to ice-cold water and the brown solid was filtered off. After treatment with a concentrated solution of sodium carbonate (20 mL), the yellow solid was collected by filtration and washed with the minimum amount of water. The compound was then dried under vacuum. Yield: 0.54 g (86%). IR: $\tilde{\nu} = 3390$ (N–H), 1630 (C=N) cm^{-1} . ^1H NMR ($[\text{D}_6]\text{DMSO}$): $\delta = 7.84$ (d, 2 H), 7.63 (d, 2 H), 7.27 (dd, 2 H), 7.15 (s, 2 H), 6.33 (s, 4 H) ppm. $\text{C}_{18}\text{H}_{12}\text{N}_6$ (312.33): calcd. C 69.22, H 3.87, N 26.91; found C 69.17, H 4.01, N 26.75.

Synthesis of DppzrBuSalH₂ (7**):** The diamino derivative **6** (94 mg, 0.3 mmol) and 3,5-di-*tert*-butylsalicylaldehyde (**3**) (188 mg, 0.8 mmol) were suspended in dry ethanol (30 mL) together with a few drops of triethyl orthoformate. The mixture was heated under reflux for 2 h and the yellow precipitate was separated by filtration. The solid was washed with diethyl ether and dried under vacuum. Yield: 192 mg (86%). IR: $\tilde{\nu} = 2950$ –2905 (C–H, aliph), 1610 (C=N) cm^{-1} . ^1H NMR (CDCl_3): $\delta = 13.26$ (s, 2 H), 9.63 (dd, 2 H), 9.30 (dd, 2 H), 8.93 (s, 2 H), 8.07 (s, 2 H), 7.82 (dd, 2 H), 7.54 (d, 2 H), 7.35 (d, 2 H), 1.48 (s, 18 H), 1.37 (s, 18 H) ppm. $\text{C}_{48}\text{H}_{52}\text{N}_6\text{O}_2$ (744.97): calcd. C 77.39, H 7.04, N 11.28; found C 77.12, H 7.17, N 11.36.

Synthesis of [DNrBuSalNi] (8**):** A solution of $\text{NiCl}_2\cdot 6\text{H}_2\text{O}$ (0.480 g, 2 mmol) in ethanol (10 mL) was added to a solution containing 4,5-diamino-1,2-dinitrobenzene (**4**) (396 mg, 2 mmol) and 3,5-di-*tert*-butylsalicylaldehyde (**3**) (936 mg, 4 mmol) in ethanol (100 mL). The resulting mixture was then heated to reflux with constant stirring for 2 h. The dark precipitate was then filtered off, washed with ethanol and dried under vacuum. Yield: 1.1 g (80%). IR (KBr): $\tilde{\nu} = 2955$ (aliphatic CH), 1619 (C=N), 1358 and 1338 cm^{-1} (NO_2). ^1H NMR (CDCl_3): $\delta = 8.23$ (s, 2 H), 8.21 (s, 2 H), 7.48 (d, 2 H), 7.14 (d, 2 H), 1.43 (s, 9 H), 1.30 (s, 9 H) ppm. $\text{C}_{36}\text{H}_{46}\text{N}_4\text{NiO}_7\cdot\text{H}_2\text{O}$ (705.47): calcd. C 61.29, H 6.57, N 7.94; found C 60.96, H 6.62, N 7.89.

Synthesis of [DArBuSalNi] (9**):** A slurry of compound **8** (690 mg, 1 mmol) and Pd/C (10%, 100 mg) in dry THF was maintained under hydrogen (40 bar) with stirring for 12 h. The mixture was filtered through a bed of Celite and then washed twice with THF ($2 \times 40 \text{ mL}$). The solvents were removed under reduced pressure and the red solid was sonicated in cold methanol (10 mL). The residue was filtered off, washed with the minimum amount of methanol and dried under vacuum. Yield: 440 mg. (70%). IR (KBr): $\tilde{\nu} = 3330$ (NH), 2950 (aliphatic CH), 1614–1596 cm^{-1} (C=N). ^1H NMR (CDCl_3): $\delta = 7.88$ (s, 2 H), 7.34 (d, 2 H), 7.02 (d, 2 H), 6.95 (s, 2 H), 3.49 (s, 4 H), 1.43 (s, 9 H), 1.37 (s, 9 H) ppm. $\text{C}_{36}\text{H}_{48}\text{N}_4\text{NiO}_2$ (627.49): calcd. C 68.91, H 7.71, N 8.93; found C 69.16, H 7.84, N 8.77.

Synthesis of DppzrBuSalNi (10): A slurry of compound **9** (628 mg, 1 mmol) in methanol (30 mL) was added dropwise to a refluxing solution of phendione (**1**) (210 mg, 1 mmol) in methanol (20 mL) with constant stirring. After the addition was complete, the mixture was heated to reflux for 2 h, whereby a red solid formed. The hot mixture was filtered and the solid was washed with methanol and dried under vacuum. Yield: 680 mg (85%). IR (KBr): $\tilde{\nu}$ = 3330 (NH), 2950 (aliphatic CH), 1614–1596 cm^{-1} (C=N). $^1\text{H NMR}$ (CDCl_3): δ = 9.49 (dd, 2 H), 9.22 (dd, 2 H), 8.39 (s, 4 H), 7.68 (dd, 2 H), 7.45 (d, 2 H), 7.14 (d, 2 H), 1.46 (s, 9 H), 1.34 (s, 9 H) ppm. $\text{C}_{48}\text{H}_{50}\text{N}_6\text{NiO}_2 \cdot 0.5\text{CH}_2\text{Cl}_2$ (844.1): calcd. C 69.01, H 6.09, N 9.96; found C 68.90, H 6.15, N 9.82.

Synthesis of $[\text{Ru}(\text{bpy})_2(\text{DppzrBuSalH}_2)](\text{PF}_6)_2$ (11): *cis*- $[\text{Ru}(\text{bpy})_2\text{Cl}_2] \cdot 2\text{H}_2\text{O}$ (52 mg, 0.1 mmol) and AgNO_3 (34 mg, 0.2 mmol) were suspended in methanol (20 mL). The mixture was stirred magnetically for 2 h under argon and a white precipitate of AgCl was filtered off. DppzrBuSalH₂ (**7**) (74 mg, 0.1 mmol) was added to the clear red solution followed by a few drops of triethyl orthoformate. The reaction mixture was heated to reflux under argon with constant stirring for 2 h. The reddish solution was filtered to remove any insoluble material and then concentrated in a rotary evaporator. An orange solid was precipitated upon addition of a concentrated aqueous solution of NH_4PF_6 . The precipitate was collected by filtration and washed with diethyl ether. Yield: 70 mg (47%). A pure sample of **11** for photophysical measurements was obtained by chromatography on neutral alumina using a mixture of dichloromethane/methanol (95:5) (R_f = 0.58). IR: $\tilde{\nu}$ = 2950–2905 (C–H, aliph), 1585–1610 (C=N) cm^{-1} . $^1\text{H NMR}$ ($[\text{D}_6]\text{DMSO}$): δ = 13.48 (s, 2 H), 9.57 (d, 2 H), 9.33 (s, 2 H), 8.88 (m, 4 H), 8.49 (s, 2 H), 8.23 (m, 4 H), 8.14 (m, 2 H), 8.05 (m, 2 H), 7.83 (m, 2 H), 7.78 (m, 2 H), 7.67 (s, 2 H), 7.60 (m, 2 H), 7.48 (s, 2 H), 7.39 (m, 2 H), 1.41 (s, 18 H), 1.33 (s, 18 H) ppm. ES-MS: m/z = 579.2 [**11**]. $\text{C}_{68}\text{H}_{68}\text{F}_{12}\text{N}_{10}\text{O}_2\text{P}_2\text{Ru} \cdot 0.33\text{NaPF}_6$ (1504.35): calcd. C 54.29, H 4.56, N 9.31; found C 54.3, H 4.7, N 9.35.

Synthesis of $[\text{Ru}(\text{bpy})_2(\text{DppzrBusalNi})](\text{PF}_6)_2$ (12): Metallation of the salophen cavity was carried out following established procedures. Ni(acetate) $_2 \cdot 4\text{H}_2\text{O}$ (6 mg, 0.24 mmol) was added to compound **11** (58 mg, 0.2 mmol) dissolved in methanol (20 mL) and the mixture was stirred for 2 h. The deep red solution was concentrated under reduced pressure and a solid was precipitated on addition of a concentrated aqueous solution of NH_4PF_6 . The red solid was filtered off, washed with water and dried under vacuum. Yield: 26 mg (85%). A pure sample of **12** for photophysical measurements was obtained by chromatography on neutral alumina using a mixture of dichloromethane/methanol (90:10) (R_f = 0.61). IR: $\tilde{\nu}$ = 2950–2905 (C–H, aliph), 1605–1640 (C=N), 845 cm^{-1} (PF_6). $^1\text{H NMR}$ ($[\text{D}_6]\text{DMSO}$): δ = 9.52 (d, 2 H), 9.33 (s, 2 H), 9.19 (s, 2 H), 8.88 (dd, 4 H), 8.22 (m, 4 H), 8.14 (m, 2 H), 8.06 (dd, 2 H), 7.82 (d, 2 H), 7.77 (d, 2 H), 7.64 (d, 2 H), 7.60 (m, 2 H), 7.41 (d, 2 H), 7.39 (m, 2 H), 1.41 (s, 18 H), 1.32 (s, 18 H) ppm. ES-MS: m/z = 607.2 [**12**]. $\text{C}_{68}\text{H}_{66}\text{F}_{12}\text{N}_{10}\text{NiO}_2\text{P}_2\text{Ru}$ (1505.01): calcd. C 54.27, H 4.42, N 9.31; found C 54.05, H 4.31, N 9.29.

Acknowledgments

The authors wish to thank Professor Jean-Jacques Girerd for fruitful discussions. This work was supported by the CNRS (Programme Energie, PRI4) and the CEA for the LRC project (LRC-CEA no. 33V). K. B. wishes to acknowledge the European TMR program and STINT (The Swedish Foundation for International Cooperation in Research and Higher Education) for financial support.

- [1] [1a] K. Kalyanasundaran, *Coord. Chem. Rev.* **1992**, *46*, 159–244. [1b] A. Juris, V. Balzani, F. Barigelletti, S. Campagna, P. Belser, A. von Zelewsky, *Coord. Chem. Rev.* **1988**, *84*, 85–277. [1c] J.-P. Sauvage, J.-P. Collin, J.-C. Chambron, S. Guillemez, C. Coudret, V. Balzani, F. Barigelletti, L. De Cola, L. Flamigni, *Chem. Rev.* **1994**, *94*, 993–1019.
- [2] [2a] J. R. Winkler, H. B. Gray, *Chem. Rev.* **1992**, *92*, 369–379. [2b] H. B. Gray, J. R. Winkler, *Annu. Rev. Biochem.* **1996**, *65*, 537–561. [2c] D. Mandler, I. Willner, *J. Am. Chem. Soc.* **1984**, *106*, 5352–5353. [2d] K. A. Maxwell, M. Sykora, J. M. De Simone, T. J. Meyer, *Inorg. Chem.* **2000**, *39*, 71–75. [2e] L. De Cola, P. Belser, *Coord. Chem. Rev.* **1998**, *177*, 301–346. [2f] C. Chiorboli, C. A. Bignozzi, F. Scandola, E. Ishow, A. Gourdon, J.-P. Launay, *Inorg. Chem.* **1999**, *38*, 2402–2410. [2g] M. D. Ward, F. Barigelletti, *Coord. Chem. Rev.* **2001**, *216*, 127–154. [2h] F. Barigelletti, L. Flamigni, *Chem. Soc. Rev.* **2000**, *29*, 1–12.
- [3] [3a] P. D. Beer, J. Cadman, *Chem. Rev.* **2000**, *205*, 131–155 and references therein. [3b] A. P. de Silva, H. Q. N. Gunaratne, T. Gunnlaugsson, A. J. M. Huxley, C. P. McCoy, J. T. Rademacher, T. E. Rice, *Chem. Rev.* **1997**, *97*, 1515–1566. [3c] T. Mizuno, W.-H. Wei, L. R. Eller, J. L. Sessler, *J. Am. Chem. Soc.* **2002**, *106*, 1134–1135. [3d] F. Bolletta, I. Costa, L. Fabbrizzi, M. Licchelli, M. Montalti, P. Pallavicini, L. Prodi, N. Zaccaroni, *J. Chem. Soc., Dalton Trans.* **1999**, 1381–1385.
- [4] [4a] J. Otsuki, M. Tsujino, T. Lizaki, K. Araki, M. Seno, K. Takatera, T. Watanabe, *J. Am. Chem. Soc.* **1997**, *119*, 7895–7896. [4b] S. Fraysse, C. Coudret, J.-P. Launay, *Eur. J. Inorg. Chem.* **2000**, 1581–1590.
- [5] K. Kalyanasundaran, *Photochemistry of Polypyridine and Porphyrin Complexes*, Academic, New York, **1992**.
- [6] [6a] N. Kitamura, H.-B. Kim, S. Sumio, S. Tazuke, *J. Phys. Chem.* **1989**, *93*, 5750–5756. [6b] H.-B. Kim, N. Kitamura, Y. Kawanishi, S. Tazuke, *J. Phys. Chem.* **1989**, *93*, 5757–5764.
- [7] [7a] G. M. Brown, N. Sutin, *J. Am. Chem. Soc.* **1979**, *101*, 883–892. [7b] M. A. Augustin, J. K. Yandell, *Inorg. Chem.* **1979**, *18*, 577–583. [7c] H. B. Gray, J. R. Winkler, *Electron Transfer in Chemistry* (Ed.: V. Balzani), Wiley-VCH, Weinheim, **2001**, vol 3, p. 3–23.
- [8] [8a] R. Langen, I.-J. Chang, J. P. Germanas, J. H. Richards, J. R. Winkler, H. B. Gray, *Science* **1995**, *268*, 1733–1735. [8b] L. Sun, L. Hammarström, B. Akermark, S. Styring, *Chem. Soc. Rev.* **2001**, *30*, 36–49. [8c] D. Burdinski, K. Wiegardt, S. Steenken, *J. Am. Chem. Soc.* **1999**, *121*, 10781–10787. [8d] D. Burdinski, E. Bothe, K. Wiegardt, *Inorg. Chem.* **2000**, *39*, 105–116. [8e] E. Fujita, S. J. Milder, B. S. Brunschwig, *Inorg. Chem.* **1992**, *30*, 2079–2035. [8f] E. Kimura, X. Bu, M. Shionoya, S. Wada, S. Maruyama, *Inorg. Chem.* **1992**, *31*, 4542–4546.
- [9] [9a] V. Balzani, A. Juris, M. Venturi, S. Campagna, S. Serroni, *Chem. Rev.* **1996**, 759–833. [9b] L. DeCola, V. Balzani, F. Barigelletti, L. Flamigni, P. Belser, S. Bernhard, *Recl. Trav. Chim. Pays Bas.* **1995**, *114*, 534. [9c] V. Balzani, F. Barigelletti, P. Belser, S. Bernhard, L. DeCola, L. Flamigni, *J. Phys. Chem.* **1996**, *100*, 16786–16788. [9d] P. Belser, S. Bernhard, C. Blum, A. Beyeler, L. DeCola, V. Balzani, *Coord. Chem. Rev.* **1999**, *192*, 155–169. [9e] A. Yoshimura, K. Nozaki, N. Ikeda, T. Ohno, *J. Phys. Chem.* **1996**, *100*, 1630. [9f] P. T. Gulyas, T. A. Smith, M. N. Paddon-Row, *J. Chem. Soc., Dalton Trans.* **1999**, 1325–1335. [9g] R. Ziessel, M. Hissler, A. El-ghayoury, A. Harriman, *Coord. Chem. Rev.* **1998**, *177*, 1251. [9h] F. Scandola, C. Chiorboli, M. T. Indelli, M. A. Rampi, *Electron Transfer in Chemistry* (Ed.: V. Balzani), Wiley-VCH, Weinheim, **2001**, vol 3, p. 337–408.
- [10] C. Kaes, A. Katz, M. W. Hosseini, *Chem. Rev.* **2000**, *100*, 3553–3590 and references therein.
- [11] [11a] A. Helms, D. Heiler, G. Mc Lendon, *J. Am. Chem. Soc.* **1991**, *113*, 4325–4327. [11b] J. Kroon, A. M. Oliver, M. N. Paddon-Row, J. W. Verhoeven, *J. Am. Chem. Soc.* **1990**, *112*, 4868–4873. [11c] E. H. Yonemoto, G. B. Saupe, R. H. Schmehl,

- S. M. Hubig, R. L. Riley, B. L. Iverson, T. E. Mallouk, *J. Am. Chem. Soc.* **1994**, *116*, 4786–4795.
- [12] N. H. Damrauer, T. R. Boussie, M. Devenney, J. K. McKusker, *J. Am. Chem. Soc.* **1997**, *119*, 8253–8268.
- [13] [13a] C. R. Rice, A. Guerrero, Z. R. Bell, R. L. Paul, G. R. Motson, J. C. Jeffery, M. D. Ward, *New J. Chem.* **2001**, *25*, 185–187. [13b] V. W.-W. Yam, V. W.-M. Lee, F. Ke, K.-W. M. Siu, *Inorg. Chem.* **1997**, *36*, 2124–2129. [13c] N. Komatsuzaki, Y. Himeda, M. Goto, K. Kasuga, H. Sugihara, H. Arakawa, *Chem. Lett.* **1999**, 327–328. [13d] K. E. Berg, Y. Pellegrin, G. Blondin, X. Ottenwaelder, Y. Journaux, M. M. Canovas, T. Mallah, S. Parsons, A. Aukauloo, *Eur. J. Inorg. Chem.* **2002**, 323–325.
- [14] [14a] J. Fees, M. Ketterle, A. Klein, J. Fiedler, W. Kaim, *J. Chem. Soc., Dalton Trans.* **1999**, 2595–2599. [14b] A. E. Friedman, J.-C. Chambron, J.-P. Sauvage, N. J. Turro, J. K. Barton, *J. Am. Chem. Soc.* **1990**, *112*, 4960–4962. [14c] J. C. Chambron, J.-P. Sauvage, E. Amouyal, P. Koffi, *Nouv. J. Chim.* **1985**, *9*, 527–529.
- [15] S. Bodige, F. M. MacDonnell, *Tetrahedron Lett.* **1997**, *38*, 8159–8160.
- [16] F. E. Arnold, *J. Polym. Sci. Polym. Chem. Ed.* **1970**, *8*, 2079–2089.
- [17] J. F. Larrow, E. N. Jacobsen, Y. Gao, Y. Hong, X. Nie, C. M. Zepp, *J. Org. Chem.* **1994**, *54*, 1939–1942.
- [18] G. W. H. Cheeseman, *J. Chem. Soc.* **1962**, 1170–1176.
- [19] B. P. Sullivan, T. J. Meyer, *Inorg. Chem.* **1978**, *17*, 3334–3341.
- [20] K. Wärnmark, J. A. Thomas, O. Heyke, J. M. Lehn, *Chem. Commun.* **1996**, 701–702.
- [21] F. Averseng, P. G Lacroix, I. Malfant, G. Lenoble, P. Cassoux, K. Nakatani, I. MalteyFanton, J. A. Delaire, A. Aukauloo, *Chem. Mater.* **1999**, *11*, 995–1002.
- [22] F. H. Allen, O. Kennard, R. Taylor, *Acc. Chem. Res.* **1983**, *16*, 146–153.
- [23] L. DeCola, V. Balzani, F. Barigelletti, L. Flamigni, P. Belser, A. von Zelewsky, M. Frank, F. Vögtle, *Inorg. Chem.* **1993**, *32*, 5228–5238.
- [24] K. Nakamoto, *Infrared and Raman Spectra of Inorganic and Coordination Compounds*, 5th ed., John Wiley & Sons, New York, **1997**.
- [25] [25a] A. B. P. Lever, *Inorganic Electronic Spectroscopy*, 2nd ed., Elsevier, New York, **1984**. [25b] C. Freire, B. de Castro, *J. Chem. Soc., Dalton Trans.* **1998**, 1491–1497.
- [26] [26a] S. D. Ernst, W. Kaim, *J. Am. Chem. Soc.* **1986**, *108*, 3578–3586. [26b] S. D. Ernst, W. Kaim, *Inorg. Chem.* **1989**, *28*, 1520–1528. [26c] J. Bolger, A. Gourdon, E. Ishow, J. P. Launay, *Inorg. Chem.* **1996**, *35*, 2937–2944. [26d] E. Ishow, A. Gourdon, J. P. Launay, C. Chiorboli, F. Scandola, *Inorg. Chem.* **1999**, *38*, 1504–1510. [26e] L. Flamigni, S. Encinas, F. Barigelletti, F. M. MacDonnell, K.-J. Kim, F. Puntoriero, S. Campagna, *Chem. Commun.* **2000**, 1185–1186. [26f] M.-J. Kim, R. Konduri, H. Ye, F. M. MacDonnell, F. Puntoriero, S. Serroni, S. Campagna, T. Holder, G. Kinsel, K. Rajeshwar, *Inorg. Chem.* **2002**, *19*, 2471–2476. [26g] R. Konduri, H. Ye, F. M. MacDonnell, S. Serroni, S. Campagna, K. Rajeshwar, *Angew. Chem.* **2002**, *17*, 3315–3317, *Angew. Chem. Int. Ed.* **2002**, *41*, 3185–3187.
- [27] J. Fees, W. Kaim, M. Moscherosch, W. Matheis, J. Klima, M. Krejcik, S. Zalis, *Inorg. Chem.* **1993**, *32*, 166–174.
- [28] W. Kaim, *Angew. Chem.* **1983**, *95*, 201–220; *Angew. Chem. Int. Ed. Engl.* **1983**, *22*, 171–190.
- [29] B. de Castro, C. Freire, *Inorg. Chem.* **1990**, *29*, 5113–5119.
- [30] [30a] A. Aukauloo, X. Ottenwaelder, R. Ruiz, Y. Journaux, S. Poussereau, B. Cervera, M. C. Muñoz, *Eur. J. Inorg. Chem.* **1999**, 1067–1071. [30b] F. V. Lovecchio, E. S. Gore, D. H. Busch, *J. Am. Chem. Soc.* **1974**, *96*, 3109–3118.
- [31] M. N. Ackermann, L. V. Interrante, *Inorg. Chem.* **1984**, *23*, 3904–3911.
- [32] [32a] G. A. Heath, L. J. Yellowlees, P. S. Braterman, *J. Chem. Soc., Chem. Commun.* **1981**, 287–289. [32b] R. M. Berger, *Inorg. Chem.* **1990**, *29*, 1920–1924.
- [33] [33a] D. E. Morris, K. W. Hanck, M. K. DeArmond, *J. Am. Chem. Soc.* **1983**, *105*, 3032–3038. [33b] W. Kaim, S. Ernst, V. Kasack, *J. Am. Chem. Soc.* **1990**, *112*, 173–178.
- [34] [34a] M. M. Richter, K. J. Brewer, *Inorg. Chem.* **1992**, *31*, 1594–1598. [34b] M. M. Richter, K. J. Brewer, *Inorg. Chem.* **1993**, *32*, 2827–2834.
- [35] The X-ray structure of the mononuclear Ni^{II} complex **10** was obtained on a microcrystal by Dr. D. Flot and Dr. C. Philouze at the ESRF facility, Grenoble, France. Owing to some disorder, an R factor of only 25% was obtained.
- [36] R. H. Holm, A. Chakravorty, L. J. Theriot, *Inorg. Chem.* **1966**, *5*, 625–635.

Received October 7, 2002

[102561]